Title

Small-Conductance Calcium-Activated Potassium Current Is Activated During Hypokalemia and Masks Short-Term Cardiac Memory Induced by Ventricular Pacing

Journal

Circulation, 132(15)

ISSN

0009-7322

Authors

Chan, Yi-Hsin
Tsai, Wei-Chung
Ko, Jum-Suk
et al.

Publication Date

2015-10-13

DOI

10.1161/circulationaha.114.015125

Peer reviewed

Small-Conductance Calcium-Activated Potassium Current Is Activated During Hypokalemia and Masks Short-Term Cardiac Memory Induced by Ventricular Pacing

Yi-Hsin Chan, MD; Wei-Chung Tsai, MD; Jum-Suk Ko, MD, PhD; Dechun Yin, MD; Po-Cheng Chang, MD; Michael Rubart, MD; James N. Weiss, MD; Thomas H. Everett IV, PhD; Shien-Fong Lin, PhD; Peng-Sheng Chen, MD

Background—Hypokalemia increases the vulnerability to ventricular fibrillation. We hypothesize that the apamin-sensitive small-conductance calcium-activated potassium current (I_{KAS}) is activated during hypokalemia and that I_{KAS} blockade is proarrhythmic.

Methods and Results—Optical mapping was performed in 23 Langendorff-perfused rabbit ventricles with atrioventricular block and either right or left ventricular pacing during normokalemia or hypokalemia. Apamin prolonged the action potential duration (APD) measured to 80% repolarization (APD_{80}) by 26 milliseconds (95% confidence interval [CI], 14–37) during normokalemia and by 54 milliseconds (95% CI, 40–68) during hypokalemia (P=0.01) at a 1000-millisecond pacing cycle length. In hypokalemic ventricles, apamin increased the maximal slope of APD restitution, the pacing cycle length threshold of APD alternans, the pacing cycle length for wave-break induction, and the area of spatially discordant APD alternans. Apamin significantly facilitated the induction of sustained ventricular fibrillation (from 3 of 9 hearts to 9 of 9 hearts; P=0.009). Short-term cardiac memory was assessed by the slope of APD_{80} versus activation time. The slope increased from 0.01 (95% CI, −0.09 to 0.12) at baseline to 0.34 (95% CI, 0.23–0.44) after apamin (P<0.001) during right ventricular pacing and from 0.07 (95% CI, −0.05 to 0.20) to 0.54 (95% CI, 0.06–1.03) after apamin infusion (P=0.045) during left ventricular pacing. Patch-clamp studies confirmed increased I_{KAS} in isolated rabbit ventricular myocytes during hypokalemia (P=0.038).

Conclusions—Hypokalemia activates I_{KAS} to shorten APD and maintain repolarization reserve at late activation sites during ventricular pacing. I_{KAS} blockade prominently lengthens the APD at late activation sites and facilitates ventricular fibrillation induction. (***Circulation*. 2015;132:1377-1386. DOI: 10.1161/CIRCULATIONAHA.114.015125.**)

Key Words: arrhythmias, cardiac ■ death, sudden, cardiac ■ ion channels

Hypokalemia is a known risk factor of sudden cardiac death.[1] Hypokalemia promotes ventricular tachyarrhythmias via multiple electrophysiological mechanisms, including prolonged ventricular repolarization, slowed conduction, steepened electric restitution, and abnormal pacemaker activity.[2] Hypokalemia directly suppresses several repolarization K^+ currents, including the inward rectifier potassium currents (I_{K1}),[3,4] rapid component of the delayed rectifier potassium currents (I_{Kr}),[5,6] and transient outward currents (I_{to}).[4] In addition, hypokalemia induces intracellular Ca^{2+} (Ca_i) overload secondary to inhibition of Na^+-K^+ pump and suppression of forward mode Na^+-Ca^{2+} exchanger.[2,3,7,8] The apamin-sensitive small-conductance calcium-activated K^+ current (I_{KAS}) is known to influence repolarization of normal atria[9,10] and in failing or infarcted ventricles.[11] In contrast, it is generally believed that I_{KAS} is not important in ventricular repolarization in normal ventricles during normokalemia.[10,12] By inducing Ca_i overload, hypokalemia might augment the conductance and trafficking of small-conductance calcium-activated K^+ (SK) channels[13] to upregulate I_{KAS} in normal ventricles. The increased I_{KAS} may

Editorial see p 1371
Clinical Perspective on p 1386

Received December 26, 2014; accepted June 11, 2015.

From Krannert Institute of Cardiology and Division of Cardiology, Department of Medicine (Y.-H.C., W.-C.T., P.-C.C., T.H.E., S.-F.L., P.-S.C.) and Wells Center for Pediatrics Research, Department of Pediatrics (M.R.), Indiana University School of Medicine, Indianapolis; Division of Cardiology, Department of Internal Medicine, Chang Gung Memorial Hospital, Chang Gung University College of Medicine, Linkou, Taoyuan, Taiwan (Y.-H.C., P.-C.C.); Division of Cardiology, Department of Internal Medicine, Kaohsiung Medical University Hospital, Kaohsiung University College of Medicine, Taiwan (W.-C.T.); Division of Cardiology, Department of Internal Medicine, Wonkwang University School of Medicine and Hospital, Jeonbuk, Republic of Korea (J.-S.K.); Department of Cardiology, First Affiliated Hospital of Harbin Medical University, China (D.Y.); Departments of Medicine (Cardiology) and Physiology, University of California, Los Angeles (J.N.W.); and Institute of Biomedical Engineering, National Chiao-Tung University, Hsin-Chu, Taiwan (S.-F.L.).

The online-only Data Supplement is available with this article at http://circ.ahajournals.org/lookup/suppl/doi:10.1161/CIRCULATIONAHA.114.015125/-/DC1.

Correspondence to Peng-Sheng Chen, MD, Krannert Institute of Cardiology, Division of Cardiology, Indiana University School of Medicine, 1800 N Capitol Ave, E475, Indianapolis, IN 46202. E-mail chenpp@iu.edu

help maintain repolarization reserve when other K currents are suppressed by hypokalemia. Blocking I_{KAS} during hypokalemia may be proarrhythmic. Because of the importance of hypokalemia in cardiac arrhythmogenesis, we investigated whether I_{KAS} is activated during hypokalemia and, if so, whether I_{KAS} blockade during hypokalemia is proarrhythmic.

Methods

Detailed methods can be found in the online-only Data Supplement.

Optical Mapping Studies

Surgical Preparation

The protocol was approved by the Institutional Animal Care and Use Committee. A total of 23 New Zealand white rabbits were used for optical mapping studies. Among them, 7 were used for normokalemic experiments, 13 for hypokalemic experiments that include 9 with right ventricular (RV) pacing and 4 with left ventricular (LV) pacing, and 3 for hypokalemia experiments during atrial pacing. The hearts were Langendorff perfused with 37°C oxygenated Tyrode solution. The composition of Tyrode solution in normokalemic experiments (n=7) was (in mmol/L) as follows: NaCl 128, KCl 4.7, $NaHCO_3$ 24, NaH_2PO_4 1.8, $CaCl_2$ 1.8, $MgCl_2$ 1.2, glucose 11.1, and bovine serum albumin 40 mg/L, pH 7.40. In hypokalemic experiments, the KCL was decreased to 2.4 mmol/L once hearts were cannulated. We then performed radiofrequency atrioventricular node ablation to reduce the ventricular rate.

Optical Mapping

We performed simultaneous optical mapping of the membrane potential (V_m) and Ca_i using techniques similar to that reported elsewhere.[14] The hearts were stained with Rhod-2 AM (Invitrogen, Grand Island, NY) for Ca_i mapping and then RH237 (Invitrogen) for V_m mapping. Blebbistatin (Tocris Bioscience, Minneapolis, MN) was used to inhibit contraction. The hearts were excited with a laser (Verdi G5, Coherent Inc, Santa Clara, CA) at a wavelength 532 nm. The signals were recorded simultaneously with 2 MiCAM Ultima cameras (BrainVision, Tokyo, Japan).

Pseudoelectrocardiogram was monitored by the use of 2 electrodes placed in the left atrium and the RV, respectively. The RV was paced at a 300-millisecond pacing cycle length (PCL) throughout the experiment except when interrupted by dynamic pacing or programmed stimulation. A dynamic pacing protocol was performed to determine the action potential duration (APD) restitution (APDR) curve. An S1/S2/S3 (short/long/short) pacing protocol and long/short coupled pacing protocol were used to simulate the ECG characteristics that initiates the early afterdepolarizations and torsades de pointes ventricular tachycardia in humans. Apamin (100 nmol/L) was then added to the perfusate, and the ventricles were continuously paced at a 300-millisecond PCL for an hour. The protocols were then repeated. Four additional hearts were studied during hypokalemia with LV pacing. Three additional hearts were paced from the right atrial appendage at a 300-millisecond PCL.

I_{KAS} Densities Determined by Voltage-Clamp Techniques

Additional rabbit hearts were used for patch-clamp studies according to previously described methods.[15] Briefly, isolated ventricular myocytes were used for whole-cell I_{KAS} recording with the voltage-clamp technique in the ruptured-patch configuration.[16] The extracellular solution contained (in mmol/L) the following: *N*-methylglucamine 140, $MgCl_2$ 1, glucose 5, HEPES 10 (pH 7.4 using HCl), and KCl 4.7 or 2.4. The internal solution consisted of (in mmol/L) the following: potassium gluconate 144, $MgCl_2$ 1.15, EGTA 5, HEPES 10, and $CaCl_2$, yielding a free-Ca^{2+} concentration of 1 μmol/L. All experiments were carried out at room temperature. Currents were elicited with the use of a voltage ramp from +40 to −100 mV (0.35 mV/s) from a holding potential of −50 mV. Voltage ramps were repeated every 10 seconds. Once the currents had stabilized, the cell was exposed to the same bath solution supplemented with apamin (100 nmol/L). Currents recorded in the presence of apamin were digitally subtracted from those measured in its absence, and the density of the apamin-sensitive current at 0 mV was calculated.

Data Analysis

APD_{80} was measured at the level of 80% repolarization of the action potential. The mean APD_{80} was calculated for all available ventricular pixels. The F/F_0 ratio was used to estimate the relative concentration of Ca_i[17] between normokalemia and hypokalemia and between early and late activation sites. Continuous variables are expressed as mean and 95% confidence interval (CI). We used the term delta to indicate the mean on the corresponding difference between 2 measures (ie, post minus pre). Paired Student *t* tests were used to compare continuous variables measured at baseline and during apamin infusion. An independent-sample *t* test was used to compare the I_{KAS} current densities with 4.7- and 2.4-mmol/L potassium concentration in the Tyrode solution. Comparison of prevalence of ventricular fibrillation (VF) inducibility between baseline and during apamin infusion was performed with the Fisher exact test. A 2-sided value of $P \leq 0.05$ was considered statistically significant.

Results

Effects of I_{KAS} Blockade on Rabbit Ventricles During Hypokalemia

The maximum Ca^{2+} F/F_0 at an LV apex during ventricular pacing at a 300-millisecond PCL was 1.12 (95% CI, 1.08–1.17; n=7) when potassium concentration was 4.7 mmol/L and increased to 1.29 (95% CI, 1.23–1.35; n=13) when the potassium concentration decreased to 2.4 mmol/L ($P<0.001$). The F/F_0 was 1.17 (95% CI, 1.14–1.20) at early activation sites and 1.29 (95% CI, 1.22–1.35; delta=0.12 [95% CI, 0.07–0.17]; $P<0.001$; n=13) at late activation sites, respectively, at baseline and 1.14 (95% CI, 1.11–1.18) and 1.27 (95% CI, 1.21–1.32) for the hypokalemic hearts (delta=0.12 [95% CI, 0.08–0.16]; $P<0.001$; n=13), respectively, after the addition of apamin. The latter findings were consistent with Ca_i accumulation at late activation sites during ventricular pacing.[18] Typical examples are shown in the Figure I in the online-only Data Supplement.

We tested the effects of apamin on 9 rabbit ventricles with RV pacing during hypokalemia [$(K^+)_0$=2.4 mmol/L]. Optical images were captured from the whole ventricle. As shown in Figure 1A, apamin prolonged APD_{80} at all PCLs during hypokalemia. However, the effects were more apparent at long than short PCLs (Figure 1B and 1C). At the PCL of 1000 and 250 milliseconds, apamin prolonged the APD_{80} from 215 milliseconds (95% CI, 205–226) to 269 milliseconds (95% CI, 250–289; delta=54 [95% CI, 40–68]; $P<0.01$) and from 173 milliseconds (95% CI, 165–180) to 189 milliseconds (95% CI, 178–199), respectively (delta=16 [95% CI, 10–22]; $P<0.01$). The average magnitudes of APD_{80} prolongation at 1000- and 250-millisecond PCLs were 54 milliseconds (95% CI, 40–68) and 16 milliseconds (95% CI, 10–22), respectively. The percentage of prolongation at PCLs of 1000 and 250 milliseconds was 25.38% (95% CI, 19.24–31.52) and 9.23% (95% CI, 6.09–12.38), respectively. We also tested the effects of apamin in 7 normokalemic ventricles [(K^+)=4.7 mmol/L]. Apamin had very little effect on APD_{80} at the 250- and 300-millisecond PCL but increased the APD_{80} by 14% at the 1000-millisecond PCL (from 182 milliseconds [95% CI, 170–194] to 208 milliseconds [95% CI, 188–227]; delta=26

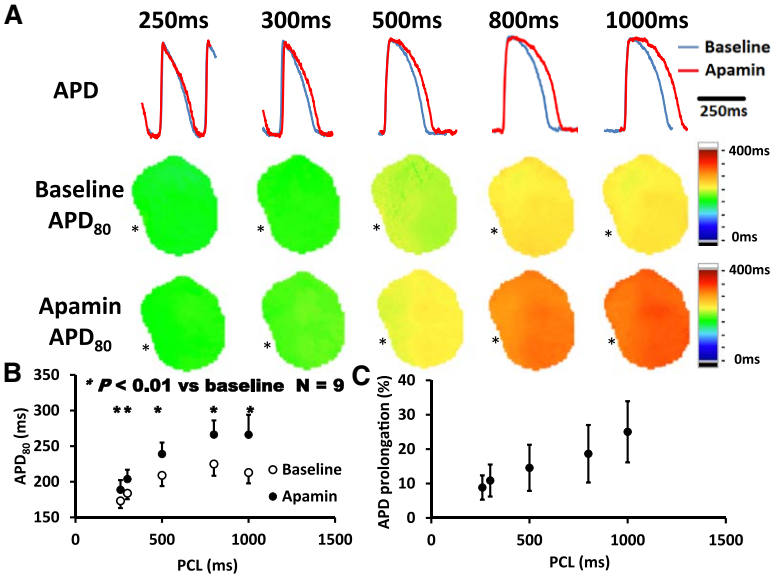

Figure 1. Effects of apamin-sensitive small-conductance calcium-activated potassium current (I_{KAS}) blockade on action potential duration (APD) at different pacing cycle lengths (PCLs) in hypokalemic ventricles. **A**, Representative membrane potential traces and APD measured to 80% repolarization (APD_{80}) maps at baseline and in the presence of apamin (100 nmol/L). The magnitude of APD prolongation was more prominent at long PCLs than at short PCLs. Asterisks mark the pacing sites. **B**, Apamin significantly prolonged APD_{80} at all PCLs, and the prolongation was more prominent at longer PCLs. *P<0.01. **C**, A plot of ΔAPD_{80} ratio ([APD_{80} after apamin minus APD_{80} at baseline]/APD_{80} at baseline) vs PCL shows that apamin prolonged APD_{80} by ≈25% at a PCL of 1000 milliseconds but only by 9% at a PCL of 250 milliseconds.

[95% CI, 14–37]; P=0.01). The average magnitude of APD_{80} prolongation at the 1000-millisecond PCL was 26 milliseconds (95% CI, 14–37), which was significantly less than that during hypokalemia (P=0.01). Figure II in the online-only Data Supplement summarizes the effects of apamin on APD in normokalemic ventricles.

APD heterogeneity has been recognized as an important factor contributing to reentrant ventricular arrhythmia. We used the standard deviation and correlation of variance generated from the optically imaged region to quantify APD heterogeneity. Figure 2A shows APD maps at baseline and after apamin and the ΔAPD maps. Figure 2B shows that apamin significantly increased the standard deviation of APD_{80} at all PCLs. Apamin also significantly increased correlation of variance of APD_{80} at 250-, 300-, and 500-millisecond PCLs. The changes in the correlation of variance at 800- and 1000-millisecond PCL were insignificant.

Effect of I_{KAS} Blockade on the Maximal Slope of APDR in Hypokalemic Ventricles

APDR curves were sampled at a basal and apical area over the LV in each heart studied. In a representative ventricle (Figure 3A), APDR slope after I_{KAS} inhibition was consistently higher than baseline at both slow (1000 milliseconds) and fast (200 milliseconds) PCL. I_{KAS} blockade also increased the maximal slope of APDR compared with baseline in both the basal and apical regions. For 9 hearts with RV pacing studied, I_{KAS} blockade increased the maximal slope of APDR from 0.99 (95% CI, 0.81–1.17) at baseline to 1.26 (95% CI, 1.04–1.47; delta=0.26 [95% CI, 0.14–0.39]; P<0.01; Figure 3B).

I_{KAS} Blockade Facilitated the Development of 2:2 Alternans and Wave Breaks in Hypokalemic Ventricles

Rapid pacing was associated with a heterogeneous distribution of APD and the calcium transient duration during

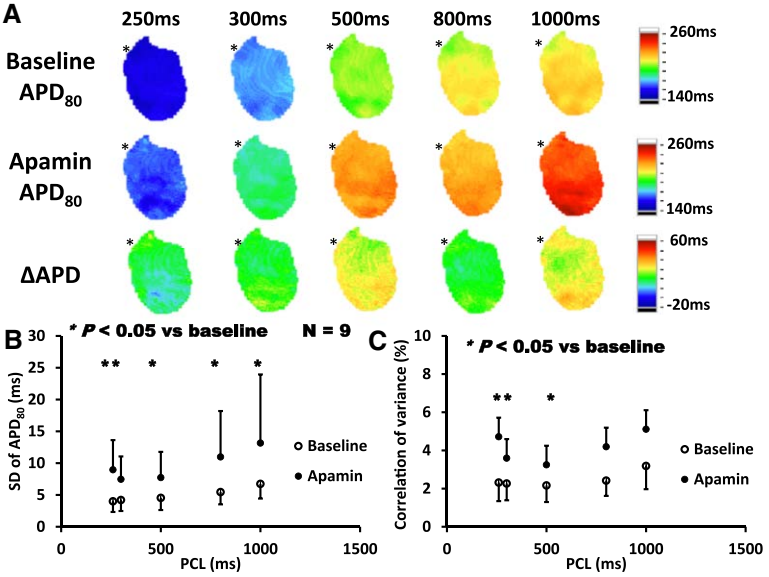

Figure 2. Effects of apamin-sensitive small-conductance calcium-activated potassium current (I_{KAS}) blockade on action potential duration (APD) measured to 80% repolarization (APD_{80}) heterogeneity at different pacing cycle lengths (PCLs) in hypokalemic ventricles. **A**, Representative APD_{80} maps at baseline (**top**) and in the presence of apamin (100 nmol/L; **middle**) and the ΔAPD map (**bottom**) at corresponding PCL. The pacing site (asterisk) was located at the right ventricular base. **B**, Apamin significantly increased the standard deviation of APD_{80} at all PCLs, and the prolongation was more prominent at longer PCLs. *P<0.05. **C**, Apamin significantly increased the correlation of variance of APD_{80} at a PCL of 250, 300, and 500 milliseconds, respectively. ΔAPD is APD_{80} after apamin minus APD_{80} at baseline. *P<0.05.

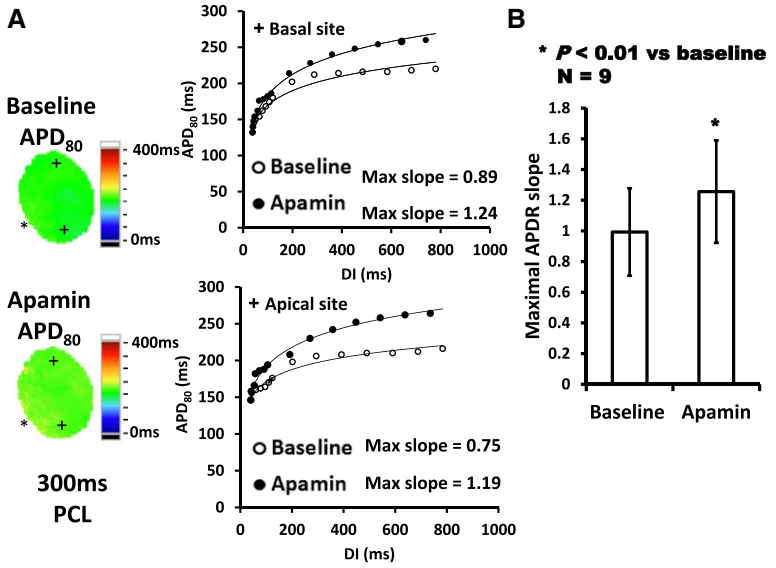

Figure 3. Effects of apamin-sensitive small-conductance calcium-activated potassium current (I_{KAS}) blockade on the maximal slope of action potential duration restitution (APDR) curve in hypokalemic ventricles. **A**, APDR curves and maximal slopes of the curves sampled at basal and apical areas of a representative ventricle. The pacing site (asterisk) was located at the right ventricular apex. **B**, Effects of apamin on the maximal slopes of APDR in normal ventricles during hypokalemia. Apamin significant increased the maximal slope of APDR curve. *P<0.01.

hypokalemia, but less so during normokalemia (Figure III in the online-only Data Supplement). In that example, calcium transient duration alternans developed at the 220-millisecond PCL, whereas both calcium transient duration and APD alternans were observed at the 190-millisecond PCL during hypokalemia, but no alternans was observed during normokalemia at 190-millisecond PCL. For all hearts studied, the longest PCL that induced calcium transient duration alternans during hypokalemia was 237 milliseconds (95% CI, 223–250), significantly longer than the longest PCL associated with APD alternans (201 milliseconds; 95% CI, 189–214; delta=36 [95% CI, 20–51]; P<0.001).

Rapid pacing caused conduction delay during hypokalemia, which was exacerbated by apamin. For 9 hypokalemic ventricles with RV pacing, apamin increased the total activation time (AT) from 26 milliseconds (95% CI, 21–31) to 36 milliseconds (95% CI, 28–43) at the 250-millisecond PCL (delta=9 [95% CI, 2–16]; P=0.014). In addition, rapid pacing causes APD alternans, especially at sites remote from the pacing site (Figure 4A). As shown in Figure 4B, the PCL threshold of alternans was significantly prolonged by apamin (250 milliseconds [95% CI, 225–274] versus 201 milliseconds [95% CI, 189–214] at baseline; delta=49 [95% CI, 20–78], P<0.01). Further decreases in PCL caused wave break in 4 ventricles (44.4%) at baseline and in all ventricles (100%) after apamin. The PCL threshold inducing wave break was also longer after the addition of apamin (186 milliseconds; 95% CI, 163–208) than at baseline (160 milliseconds; 95% CI, 147–173; delta=26 [95% CI, 11–40]; P<0.01).

APD alternans was initially concordant but became discordant when PCL was shortened. Figure 5 shows examples of discordant alternans induced by rapid pacing at baseline and after apamin. To quantify the degree of spatially discordant APD alternans in each ventricle, we calculated the total pixel numbers showing discordant alternans before and after apamin infusion at the shortest PCL that allowed 1:1

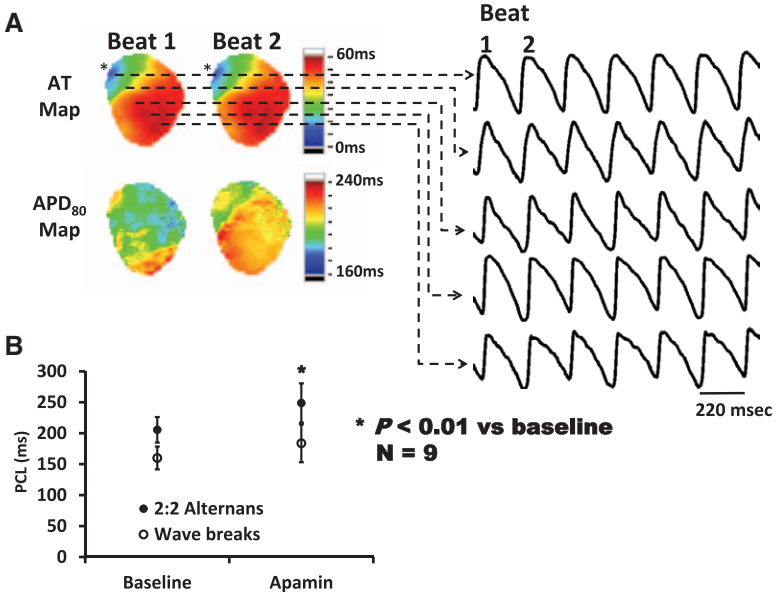

Figure 4. Development of 2:2 alternans and wave breaks after apamin-sensitive small-conductance calcium-activated potassium current (I_{KAS}) blockade. **A**, Representative trace of 2:2 alternans in a representative hypokalemic ventricle after apamin infusion. Corresponding activation time (AT) and action potential duration (APD) maps from beats 1 and 2 are shown. Note there is an obvious 2:2 alternans at the remote activation site. The pacing site is located at the right ventricular base (asterisk). **B**, Apamin prolonged the pacing cycle length (PCL) threshold of 2:2 alternans and wave breaks. Wave breaks could be induced in only 4 ventricles (44.4%). After I_{KAS} blockade, 9 ventricles (100%) developed 2:2 alternans, and all showed wave breaks at shorter PCLs. *P<0.01.

capture. At baseline, 4 ventricles (44.4%) showed small areas of spatially discordant APD alternans at 140- to 200-millisecond PCLs. Apamin facilitated the formation of spatially discordant APD alternans by lengthening the nodal line and enlarging the area involved in alternans (Figure 5A). For all 9 hypokalemic hearts with RV pacing, apamin significantly increased the area ratio (percent of mapped region) of spatially discordant APD alternans from 7.89% (95% CI, −0.46 to 16.23) to 45.3% (95% CI, 32.86–57.81) at the shortest PCL that allowed 1:1 capture (delta=37.44% [95% CI, 27.21–47.69]; P<0.001; Figure 5B). Further decreasing the PCL resulted in wave break in 4 ventricles at baseline and in all 9 ventricles after apamin.

I_{KAS} Blockade and Activation-Repolarization Coupling

Activation-repolarization coupling was assessed by plotting APD_{80} against the AT during pacing. The PCL used for these analyses was 300 milliseconds. Representative plots of APD_{80} versus AT in 2 hearts with different RV pacing sites are shown in Figure 6A and 6B. The slope of APD to AT was flat at baseline. Apamin caused more APD prolongation at late activation sites than early activation sites, leading to increased APD-to-AT slope. There was a negative correlation of ΔAPD_{80} (APD_{80} after apamin minus that at baseline) versus baseline APD_{80}. For all 9 hearts with RV pacing during hypokalemia, apamin increased the APD-to-AT slope from 0.01 (95% CI, −0.09 to 0.12) to 0.34 (95% CI, 0.23–0.44; delta=0.32 [95% CI, 0.19–0.45]; P<0.001). We measured the APD-to-AT slope in 4 hypokalemic ventricles studied with recordings available at both 30 and 90 minutes after apamin administration. The APD-to-AT slopes at 30 and 90 minutes were 0.30 (95% CI, 0.25–0.35) and 0.32 (95% CI, 0.19–0.45), respectively (P=0.98), indicating a stable APD-to-AT relationship (Figure 7).

We also tested the effect of activation-repolarization coupling in 4 additional ventricles paced from the LV base. A representative plot of APD_{80} versus AT in 1 heart with LV base pacing is shown in Figure IV in the online-only Data Supplement. For 4 hearts paced from the LV base, apamin increased the APD-to-AT slope from 0.07 (95% CI, −0.05 to 0.20) at baseline to 0.54 (95% CI, 0.06–1.03; delta=0.47 [95% CI, 0.02–0.93]; P=0.045).

Effects of Apamin in Atrially Paced Hearts

The APD_{80} at the 300-millisecond PCL at baseline was 153 milliseconds (95% CI, 128–178). Apamin prolonged the APD_{80} to 176 milliseconds (95% CI, 143–208; delta=23 [95% CI, 7–39]; P=0.024). The entire epicardium was activated within 13 milliseconds (95% CI, 6–21) at baseline and 17 milliseconds (95% CI, 6–27; delta=3 [95% CI, 0–6]; P=0.038) after apamin. Although apamin increased AT, it did not change the ventricular activation sequence. The APD-to-AT slope in these 3 hearts was 0.98 (95% CI, −2.61 to 4.58) at baseline and −0.22 (95% CI, −1.57 to 1.13) after apamin (delta=−1.20 [95% CI, −4.62 to 2.23]; P=0.271). A representative response to apamin is shown in Figure V in the online-only Data Supplement.

Effects of Hypokalemia on I_{KAS} Current Density

We successfully completed patch-clamp studies in isolated rabbit ventricular myocytes with the potassium concentration

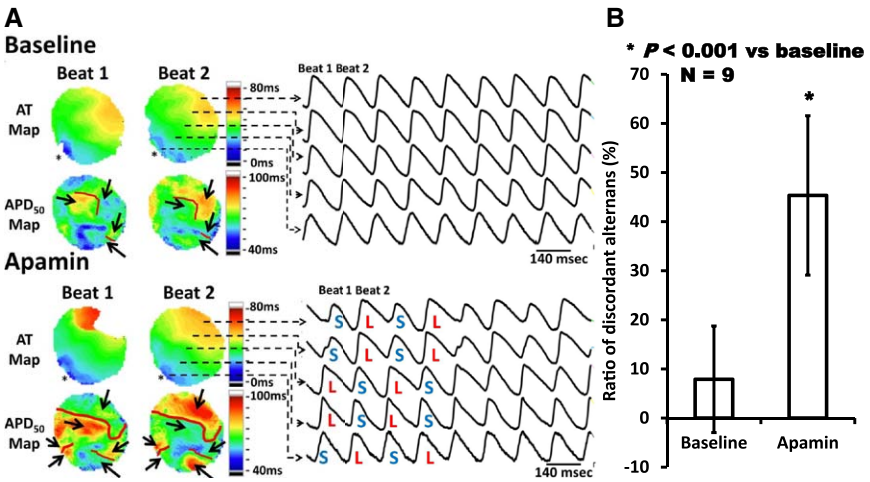

Figure 5. Development of spatially discordant action potential duration (APD) alternans in hypokalemic ventricles after apamin-sensitive small-conductance calcium-activated potassium current (I_{KAS}) blockade. **A**, **Top**, Corresponding activation time (AT) and APD maps from beats 1 and 2 at baseline with a 140-millisecond pacing cycle length (PCL). Some small areas showed spatially discordant APD alternans within the whole optical area (arrowheads). The red line indicates the nodal line. The 5 APD tracings sampled from the pacing site to a remote site consecutively showed no obvious discordant APD alternans (arrowheads). **Bottom**, Corresponding AT and APD maps from beats 1 and 2 are shown after apamin under the same PCL. Note that the area of discordant APD alternans was increased compared with baseline (arrows). The red line indicates the nodal line. It is noted that the 5 APD tracings sampled from the pacing site to a remote site consecutively showed discordant APD alternans after apamin infusion (arrowheads). There was wave-break formation followed by ventricular fibrillation when the PCL was further decreased to 140 milliseconds. The pacing site (asterisk) was located at the right ventricular apex. **B**, Effects of I_{KAS} blockade on the formation of spatially discordant APD alternans in all hypokalemic ventricles (n=9). I_{KAS} blockade significantly increased the area ratio of discordant APD alternans to whole optical areas compared with baseline. L indicates long APD; and S, short APD. *P<0.001.

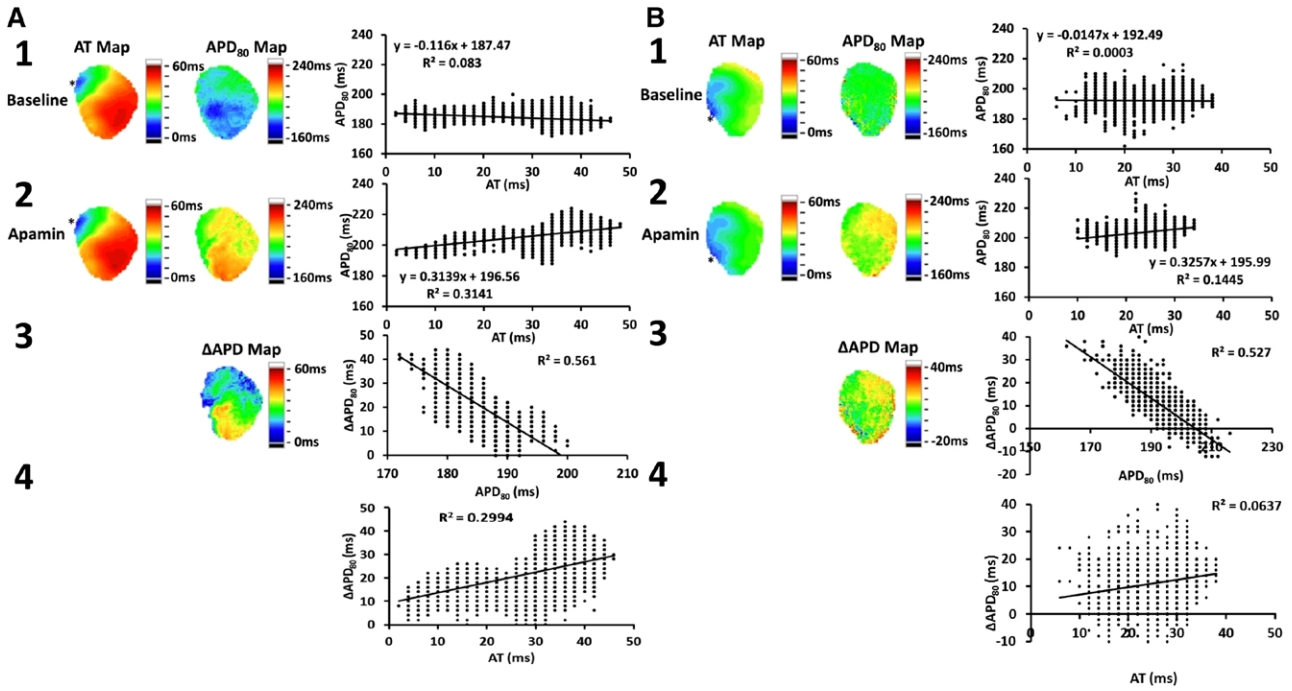

Figure 6. Effects of apamin-sensitive small-conductance calcium-activated potassium current (I_{KAS}) blockade on the relation of action potential duration (APD) to activation time (AT) on the epicardium determined during right ventricular (RV) pacing at a 300-millisecond pacing cycle length (PCL) in hypokalemic ventricles. **A**, The AT maps, APD maps, and corresponding plot of the APD-AT relationship at baseline (1) and after apamin infusion (2) in 1 ventricle. The pacing site (asterisk) was located at the RV base. Apamin increased the APD-AT slope from −0.12 to 0.32. (3) The ΔAPD map and correlation between ΔAPD and baseline APD_{80} in the ventricle at a 300-millisecond PCL. (4) The corresponding ΔAPD-AT plot at a PCL of 300 milliseconds. **B**, The AT maps, APD maps, and corresponding plot of the APD-AT relationship at baseline (1) and after apamin infusion (2) in another ventricle during the 300-millisecond PCL. The pacing site is located at the RV apex (asterisk). Apamin increased the APD-AT slope from −0.01 to 0.33. (3) The ΔAPD map and correlation between ΔAPD and baseline APD_{80} in the ventricle at a 300-millisecond PCL. (4) The corresponding ΔAPD-AT plot at a PCL of 300 milliseconds. ΔAPD is APD_{80} after apamin minus APD_{80} at baseline.

at 4.7 mmol/L (n=3) and 2.4 mmol/L (n=3) in the Tyrode solution. The densities of I_{KAS} were 0.04 pA/pF (95% CI, −0.04 to 0.12) and 2.20 pA/pF (95% CI, 0.33–4.06), respectively (delta=2.16 [95% CI, 0.30–4.02]; P=0.038). An example of the patch-clamp study is shown in Figure VI in the online-only Data Supplement.

I_{KAS} Blockade Increased Ventricular Vulnerability to Fibrillation in Hypokalemic Ventricles

No spontaneous tachyarrhythmias were observed during the study. Rapid pacing induced VF episodes in 3 of 9 ventricles (33.3%) studied at baseline. VF episodes were successfully induced in all 9 ventricles (100%) after apamin infusion

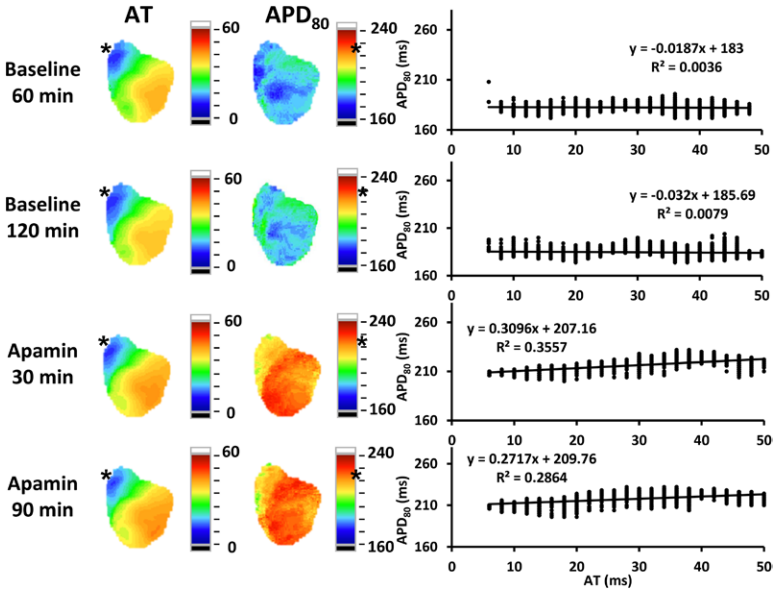

Figure 7. Relationship of action potential duration (APD) to activation time (AT) over time. The rabbit ventricles were paced from the right ventricle (RV; asterisk) at a 300-millisecond pacing cycle length (PCL). Maps were obtained at different times of the experiment as labeled on the **left**. The sequence of activation on the left ventricle was stable over time. The APD measured to 80% repolarization (APD_{80}) at baseline was stable for 2 hours. After the addition of apamin, the APD_{80} was lengthened, and the APD-to-AT slope increased at 30 minutes. These changes were stable 1 hour later. The pacing site (asterisk) is located at the RV base.

(P=0.009). In all, there were 8 and 43 VF episodes at baseline and after apamin infusion, respectively. Figure 8A shows phase maps indicating phase singularities (black arrows) during VF episodes at baseline and after I_{KAS} blockade in a representative ventricle. I_{KAS} blockade increased the number of phase singularities of VF episodes (P=0.001; Figure 8B). The short/long/short or long/short coupled pacing protocol did not induce any VF episodes at baseline during hypokalemia. However, VF episodes were successfully induced in 7 ventricles (77.8%) by short/long/short or long/short coupled pacing protocol after apamin infusion (P=0.002). Representative recording of optical mapping in 1 heart revealed that apamin increased the slope of APD to AT from −0.04 to 0.49 at a PCL of 1000 milliseconds compared with baseline (Figure VIIA in the online-only Data Supplement). The premature stimulation (230 milliseconds coupling interval) captured the tissue near pacing site. However, because of the prolongation of APD remote from pacing site, the impulse was blocked half-way through the ventricle, leading to reentry and VF (Figure VIIB in the online-only Data Supplement).

Discussion

We found that hypokalemia activated I_{KAS} in normal ventricles with atrioventricular block. The effect on APD was greater at longer PCL than at shorter PCL. Blockade of I_{KAS} by apamin under these conditions was proarrhythmic, suggesting that I_{KAS} activation plays an important role in protecting ventricular repolarization reserve and in preventing the development of sustained ventricular arrhythmias of the nonfailing ventricles. In addition, apamin unmasked a positive correlation between ΔAPD and AT, indicating that pacing-induced cardiac memory is also modulated by I_{KAS}.

Mechanisms of Cardiac Memory

Cardiac memory is a term coined by Rosenbaum et al[19] to describe a specialized form of remodeling characterized by an altered T wave recorded induced by a preceding period of altered electric activation.[20] In the heart, short-term memory refers to the effects of pacing history on the APD and should be distinguished from long-term memory related to changes in gene expression causing electric remodeling.[21] Short-term cardiac memory may be mediated by angiotensin activation induced by altered myocardial stretch during pacing.[22] Angiotensin receptor type 1 forms a complex with the transient outward potassium channel Kv4.3 and regulates its gating properties and intracellular localization.[23] Because transient outward current (I_{to}) is important in the generation of cardiac memory,[24,25] angiotensin activation leads to a loss of epicardial $I_{to,}$[26] an altered apicobasal repolarization gradient, and T-wave changes.[27] The short-term cardiac memory can also be induced in rabbit ventricles by 5 minutes of ventricular pacing that returned to control in 5 to 10 minutes.[28] However, losartan, an angiotensin receptor type 1 blocker, did not influence the expression of memory in that study. The native rabbit ventricular I_{to1} (chiefly $I_{to1,s}$ encoded by Kv1.4) has an unusually long time constant of recovery from inactivation.[29] Thus, I_{to1} is almost completely inactivated and makes a negligible contribution to the AP at a PCL of <1 second. I_{KAS} acts like an I_{to} in that its conductance tracks the Ca^{2+} transient. It is possible that, in the rabbit ventricles paced at a 300-millisecond PCL, I_{KAS} could form the basis of the memory effect rather than I_{to}.

I_{KAS} and Cardiac Memory

The induction of cardiac memory in rabbit ventricles can be detected from the relationship between APD and AT.[30] During sinus rhythm or atrial pacing, ventricular APD varies inversely with respect to AT. During ventricular pacing, however, the negative correlation is replaced by a positive correlation lasting ≈60 minutes, after which the negative correlation re-establishes itself. Subsequent studies have suggested that ventricular pacing induces cardiac memory through a mechanoelectric feedback mechanism[31] related to altered sarcomeric Ca^{2+} handling and cytosolic Ca^{2+} accumulation at sites remote from the pacing site.[18] That mechanism could potentially explain our findings if the increased Ca_i at remote sites activates inward currents that prolong APD but are compensated for by activation of I_{KAS}, which attenuates APD prolongation. By inhibiting I_{KAS}, apamin unmasks APD prolongation at remote sites, revealing the underlying positive correlation between APD

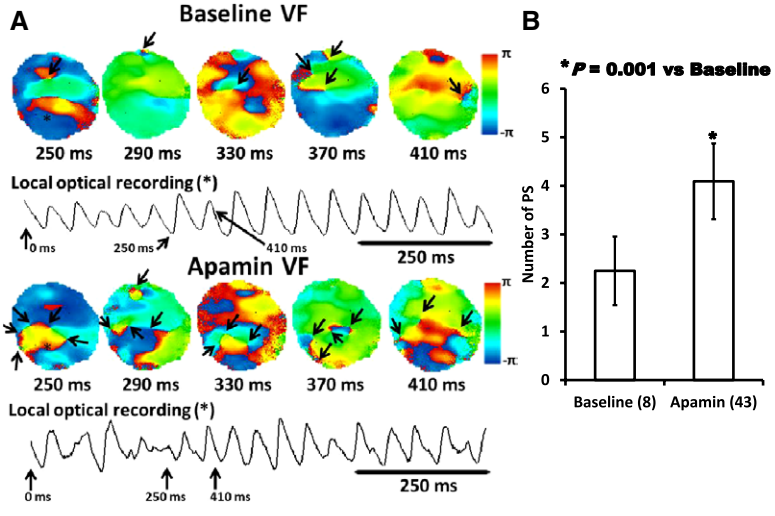

Figure 8. Effects of apamin-sensitive small-conductance calcium-activated potassium current (I_{KAS}) blockade on the wave breaks of ventricular fibrillation (VF) episodes in hypokalemic ventricles. **A**, Consecutive phase maps sampled at 40 milliseconds during VF at baseline and after apamin infusion in a representative ventricle. Phase singularities (PSs; wave breaks) are indicated by black arrows. The optical signals during VF came from a site marked by an asterisk. **B**, Effects of apamin on the number of phase singularities in all VF episodes before and after apamin infusion. Note that the phase singularities were significantly increased by apamin infusion. *P=0.001.

and AT as a reflection of short-term cardiac memory. Our data therefore suggest that short-term cardiac memory induced by ventricular pacing is strongly modulated by I_{KAS}.

Importance of Short-Term Cardiac Memory to Ventricular Arrhythmogenesis

The safety factor of propagation is determined in part by the spatial patterns of repolarization.[32] Propagation from areas with short APD into areas with long APD is associated with a reduced safety factor of propagation, increasing the propensity for conduction block and reentry. Because pacing-induced short-term cardiac memory is associated with greater APD prolongation remote from the pacing site than close to the pacing site, the safety factor of propagation is reduced particularly during premature depolarization. Consistent with this hypothesis, we have shown that apamin administration makes it easier for a premature stimulation to induce wave breaks.

Another form of cardiac memory is the rate- or diastolic interval–dependent changes in APDR.[33] This type of memory is dependent on the kinetic properties of multiple different ion channels. A previous study[34] and the present study indicated that I_{KAS} is important in APDR. In computer simulations, adding a potassium memory current to the Luo-Rudy model showed that the accumulation of the memory potassium current played an important role in the progression of the activation patterns of VF over time by progressively shortening the APD.[21] I_{KAS} activation as Ca overload develops during early VF could act in the same way as a memory K current and thus influences the generation and maintenance of VF.[34,35]

I_{KAS} and the Repolarization Reserve

Despite significant APD prolongation during moderate hypokalemic ventricles after I_{KAS} inhibition, spontaneous early afterdepolarizations or torsades de pointes were not observed. However, in case of associated disease conditions such as heart failure and coexistent atrioventricular block and bradycardia, spontaneous early afterdepolarizations or torsades de pointes may occur after apamin.[14] Another possible explanation is that I_{Ks} and I_{Kr} are activated during the phase 3 of the action potential, whereas I_{KAS} is most important during the phase 2 of the action potential when $I_{Ca,L}$ activity, sarcoplasmic Ca^{2+} release, and the Ca_i are high. The effects of I_{KAS} blockade may be sufficient to prolong the APD. However, without other associated ionic current changes, APD prolongation by itself is insufficient to induce early afterdepolarizations or torsades de pointes.[36]

I_{KAS} Blockade Increases Tissue Vulnerability in Hypokalemic Ventricles

We observed increased APD heterogeneity, steepened maximal slope of APDR, increased PCL threshold for alternans, and increased spatially discordant APD alternans after I_{KAS} inhibition, factors that increase vulnerability to ventricular arrhythmias.[33,37,38] The out-of-phase regions of discordant APD alternans are separated by a nodal line[39] in which the spatial gradients in APD or Ca_i transient amplitude are the steepest, predisposing to localized conduction block.[33,40] The augmentation of spatially discordant APD alternans by I_{KAS} blockade in our study can be explained by 2 mechanisms: I_{KAS} blockade steepened the APDR curve in hypokalemic ventricles, which would facilitate the formation of discordant APD alternans.[33] In addition, because V_m and Ca_i are bidirectionally coupled in myocardial tissue, I_{KAS} may play an important role to modulate the V_m and Ca_i coupling. Longer Ca_i transient results in greater I_{KAS} activation to compensate for the longer APD caused by longer Ca_i transient. Therefore, I_{KAS} inhibition would amplify the effect of Ca^{2+} on APD prolongation and hence prolong the PCL threshold for alternans.

Study Limitations

The optical mapping techniques do not allow us to determine the absolute levels of the Ca_i. Therefore, we relied on reports by others to support the altered Ca_i handling at late activated regions.[18] We showed that I_{KAS} blockade facilitated ventricular arrhythmias in hypokalemic normal ventricles, a finding opposite to that in failing ventricles, in which apamin was antifibrillatory.[34] The mechanisms of the opposite observations may be related to additional remodeling changes that are present in failing but not normal ventricles. Apamin has been reported to also block the fetal-type $I_{Ca,L,}$[41] implying that it is not a specific ion channel blocker. However, Yu et al[16] recently showed that apamin is a highly specific I_{KAS} blocker for human type cardiac ion channels and does not block $I_{Ca,L.}$

Summary and Clinical Significance

A large study involving 58 167 hospital inpatients showed that 5.2% had serum potassium <3.0 mmol/l, including 73 patients with potassium <2.0 mmol/L and 472 patients with potassium between 2.0 and 2.4 mmol/L.[42] Hypokalemia significantly increases mortality in hospitalized patients.[42] We showed that I_{KAS} blockade increased the vulnerability to ventricular tachyarrhythmias in hypokalemic ventricles. I_{KAS} also plays an important role in modulating cardiac memory. These findings indicate that I_{KAS} is important in ventricular arrhythmogenesis during hypokalemia. This may be relevant to drug safety because a number of commonly used clinical drugs such as anesthetic agents,[43] quinine, *d*-tubocurarine,[44] and amiodarone[45] are known inhibitors of I_{KAS}. It is possible that further investigations will discover the I_{KAS}-blocking action of other drugs used commonly in clinical practice. The I_{KAS}-blocking action may contribute to their proarrhythmic mechanism. Better understanding the drug effects on I_{KAS} may be important in the prevention of sudden death and promote drug safety in patients with severe hypokalemia.

Acknowledgments

We thank Nicole Courtney, Christopher Corr, David Adams, and David Wagner for their assistance.

Sources of Funding

This work was supported by National Institutes of Health grants P01 HL78931, R01 HL71140, and R41HL124741; a Medtronic-Zipes Endowment of the Indiana University; and the Indiana University Health–Indiana University School of Medicine Strategic Research Initiative.

Disclosures

Shien-Fong Lin and Peng-Sheng Chen have equity interest in Arrhythmotech, LLC. Their laboratory receives equipment donations from Medtronic, St. Jude and Cyberonics Inc. The other authors report no conflicts.

References

1. Zipes DP, Wellens HJ. Sudden cardiac death. *Circulation*. 1998;98:2334–2351.
2. Osadchii OE. Mechanisms of hypokalemia-induced ventricular arrhythmogenicity. *Fundam Clin Pharmacol*. 2010;24:547–559. doi: 10.1111/j.1472-8206.2010.00835.x.
3. Bouchard R, Clark RB, Juhasz AE, Giles WR. Changes in extracellular K+ concentration modulate contractility of rat and rabbit cardiac myocytes via the inward rectifier K+ current IK1. *J Physiol*. 2004;556(pt 3):773–790. doi: 10.1113/jphysiol.2003.058248.
4. Killeen MJ, Gurung IS, Thomas G, Stokoe KS, Grace AA, Huang CL. Separation of early afterdepolarizations from arrhythmogenic substrate in the isolated perfused hypokalaemic murine heart through modifiers of calcium homeostasis. *Acta Physiol (Oxf)*. 2007;191:43–58. doi: 10.1111/j.1748-1716.2007.01715.x.
5. Yang T, Snyders DJ, Roden DM. Rapid inactivation determines the rectification and (K+)o dependence of the rapid component of the delayed rectifier K+ current in cardiac cells. *Circ Res*. 1997;80:782–789.
6. Guo J, Massaeli H, Xu J, Jia Z, Wigle JT, Mesaeli N, Zhang S. Extracellular K+ concentration controls cell surface density of I_{Kr} in rabbit hearts and of the HERG channel in human cell lines. *J Clin Invest*. 2009;119:2745–2757. doi: 10.1172/JCI39027.
7. Weiss JN. Palpitations, potassium and the pump. *J Physiol*. 2015;593:1387–1388. doi: 10.1113/jphysiol.2014.285924.
8. Aronsen JM, Skogestad J, Lewalle A, Louch WE, Hougen K, Stokke MK, Swift F, Niederer S, Smith NP, Sejersted OM, Sjaastad I. Hypokalaemia induces Ca(2+) overload and Ca(2+) waves in ventricular myocytes by reducing Na(+),K(+)-ATPase α2 activity. *J Physiol*. 2015;593:1509–1521. doi: 10.1113/jphysiol.2014.279893.
9. Tuteja D, Xu D, Timofeyev V, Lu L, Sharma D, Zhang Z, Xu Y, Nie L, Vázquez AE, Young JN, Glatter KA, Chiamvimonvat N. Differential expression of small-conductance Ca^{2+}-activated K+ channels SK1, SK2, and SK3 in mouse atrial and ventricular myocytes. *Am J Physiol Heart Circ Physiol*. 2005;289:H2714–H2723. doi: 10.1152/ajpheart.00534.2005.
10. Xu Y, Tuteja D, Zhang Z, Xu D, Zhang Y, Rodriguez J, Nie L, Tuxson HR, Young JN, Glatter KA, Vázquez AE, Yamoah EN, Chiamvimonvat N. Molecular identification and functional roles of a Ca(2+)-activated K+ channel in human and mouse hearts. *J Biol Chem*. 2003;278:49085–49094. doi: 10.1074/jbc.M307508200.
11. Chang PC, Chen PS. SK channels and ventricular arrhythmias in heart failure. *Trends Cardiovasc Med*. 2015;25:508–514. doi: 10.1016/j.tcm.2015.01.010..
12. Nagy N, Szuts V, Horváth Z, Seprényi G, Farkas AS, Acsai K, Prorok J, Bitay M, Kun A, Pataricza J, Papp JG, Nánási PP, Varró A, Tóth A. Does small-conductance calcium-activated potassium channel contribute to cardiac repolarization? *J Mol Cell Cardiol*. 2009;47:656–663. doi: 10.1016/j.yjmcc.2009.07.019.
13. Rafizadeh S, Zhang Z, Woltz RL, Kim HJ, Myers RE, Lu L, Tuteja D, Singapuri A, Bigdeli AA, Harchache SB, Knowlton AA, Yarov-Yarovoy V, Yamoah EN, Chiamvimonvat N. Functional interaction with filamin A and intracellular Ca^{2+} enhance the surface membrane expression of a small-conductance Ca^{2+}-activated K+ (SK2) channel. *Proc Natl Acad Sci USA*. 2014;111:9989–9994. doi: 10.1073/pnas.1323541111.
14. Chang PC, Hsieh YC, Hsueh CH, Weiss JN, Lin SF, Chen PS. Apamin induces early afterdepolarizations and torsades de pointes ventricular arrhythmia from failing rabbit ventricles exhibiting secondary rises in intracellular calcium. *Heart Rhythm*. 2013;10:1516–1524. doi: 10.1016/j.hrthm.2013.07.003.
15. Ahmmed GU, Xu Y, Hong Dong P, Zhang Z, Eiserich J, Chiamvimonvat N. Nitric oxide modulates cardiac Na(+) channel via protein kinase A and protein kinase G. *Circ Res*. 2001;89:1005–1013.
16. Yu CC, Ai T, Weiss JN, Chen PS. Apamin does not inhibit human cardiac Na^+ current, L-type Ca^{2+} current or other major K^+ currents. *PLoS One*. 2014;9:e96691. doi: 10.1371/journal.pone.0096691.
17. Tsai CT, Wang DL, Chen WP, Hwang JJ, Hsieh CS, Hsu KL, Tseng CD, Lai LP, Tseng YZ, Chiang FT, Lin JL. Angiotensin II increases expression of alpha1C subunit of L-type calcium channel through a reactive oxygen species and cAMP response element-binding protein-dependent pathway in HL-1 myocytes. *Circ Res*. 2007;100:1476–1485. doi: 10.1161/01.RES.0000268497.93085.e1.
18. Jeyaraj D, Wan X, Ficker E, Stelzer JE, Deschenes I, Liu H, Wilson LD, Decker KF, Said TH, Jain MK, Rudy Y, Rosenbaum DS. Ionic bases for electrical remodeling of the canine cardiac ventricle. *Am J Physiol Heart Circ Physiol*. 2013;305:H410–H419. doi: 10.1152/ajpheart.00213.2013.
19. Rosenbaum MB, Blanco HH, Elizari MV, Lázzari JO, Davidenko JM. Electrotonic modulation of the T wave and cardiac memory. *Am J Cardiol*. 1982;50:213–222.
20. Patberg KW, Shvilkin A, Plotnikov AN, Chandra P, Josephson ME, Rosen MR. Cardiac memory: mechanisms and clinical implications. *Heart Rhythm*. 2005;2:1376–1382. doi: 10.1016/j.hrthm.2005.08.021.
21. Baher A, Qu Z, Hayatdavoudi A, Lamp ST, Yang MJ, Xie F, Turner S, Garfinkel A, Weiss JN. Short-term cardiac memory and mother rotor fibrillation. *Am J Physiol Heart Circ Physiol*. 2007;292:H180–H189. doi: 10.1152/ajpheart.00944.2005.
22. Ozgen N, Rosen MR. Cardiac memory: a work in progress. *Heart Rhythm*. 2009;6:564–570. doi: 10.1016/j.hrthm.2009.01.008.
23. Doronin SV, Potapova IA, Lu Z, Cohen IS. Angiotensin receptor type 1 forms a complex with the transient outward potassium channel Kv4.3 and regulates its gating properties and intracellular localization. *J Biol Chem*. 2004;279:48231–48237. doi: 10.1074/jbc.M405789200.
24. Ricard P, Danilo P Jr, Cohen IS, Burkhoff D, Rosen MR. A role for the renin-angiotensin system in the evolution of cardiac memory. *J Cardiovasc Electrophysiol*. 1999;10:545–551.
25. del Balzo U, Rosen MR. T wave changes persisting after ventricular pacing in canine heart are altered by 4-aminopyridine but not by lidocaine: implications with respect to phenomenon of cardiac "memory." *Circulation*. 1992;85:1464–1472.
26. Yu H, Gao J, Wang H, Wymore R, Steinberg S, McKinnon D, Rosen MR, Cohen IS. Effects of the renin-angiotensin system on the current *I*(to) in epicardial and endocardial ventricular myocytes from the canine heart. *Circ Res*. 2000;86:1062–1068.
27. Janse MJ, Sosunov EA, Coronel R, Opthof T, Anyukhovsky EP, de Bakker JM, Plotnikov AN, Shlapakova IN, Danilo P Jr, Tijssen JG, Rosen MR. Repolarization gradients in the canine left ventricle before and after induction of short-term cardiac memory. *Circulation*. 2005;112:1711–1718. doi: 10.1161/CIRCULATIONAHA.104.516583.
28. Sosunov EA, Anyukhovsky EP, Rosen MR. Altered ventricular stretch contributes to initiation of cardiac memory. *Heart Rhythm*. 2008;5:106–113. doi: 10.1016/j.hrthm.2007.09.008.
29. Zhao Z, Xie Y, Wen H, Xiao D, Allen C, Fefelova N, Dun W, Boyden PA, Qu Z, Xie LH. Role of the transient outward potassium current in the genesis of early afterdepolarizations in cardiac cells. *Cardiovasc Res*. 2012;95:308–316. doi: 10.1093/cvr/cvs183.
30. Costard-Jäckle A, Goetsch B, Antz M, Franz MR. Slow and long-lasting modulation of myocardial repolarization produced by ectopic activation in isolated rabbit hearts: evidence for cardiac "memory." *Circulation*. 1989;80:1412–1420.
31. Jeyaraj D, Wilson LD, Zhong J, Flask C, Saffitz JE, Deschênes I, Yu X, Rosenbaum DS. Mechanoelectrical feedback as novel mechanism of cardiac electrical remodeling. *Circulation*. 2007;115:3145–3155. doi: 10.1161/CIRCULATIONAHA.107.688317.
32. Spach MS, Dolber PC, Heidlage JF. Interaction of inhomogeneities of repolarization with anisotropic propagation in dog atria: a mechanism for both preventing and initiating reentry. *Circ Res*. 1989;65:1612–1631.
33. Weiss JN, Karma A, Shiferaw Y, Chen PS, Garfinkel A, Qu Z. From pulsus to pulseless: the saga of cardiac alternans. *Circ Res*. 2006;98:1244–1253. doi: 10.1161/01.RES.0000224540.97431.f0.
34. Hsieh YC, Chang PC, Hsueh CH, Lee YS, Shen C, Weiss JN, Chen Z, Ai T, Lin SF, Chen PS. Apamin-sensitive potassium current modulates action potential duration restitution and arrhythmogenesis of failing rabbit ventricles. *Circ Arrhythm Electrophysiol*. 2013;6:410–418. doi: 10.1161/CIRCEP.111.000152.
35. Chua SK, Chang PC, Maruyama M, Turker I, Shinohara T, Shen MJ, Chen Z, Shen C, Rubart-von der Lohe M, Lopshire JC, Ogawa M, Weiss JN, Lin SF, Ai T, Chen PS. Small-conductance calcium-activated potassium channel and recurrent ventricular fibrillation in failing rabbit ventricles. *Circ Res*. 2011;108:971–979. doi: 10.1161/CIRCRESAHA.110.238386.
36. Hondeghem LM, Dujardin K, De Clerck F. Phase 2 prolongation, in the absence of instability and triangulation, antagonizes class III proarrhythmia. *Cardiovasc Res*. 2001;50:345–353.
37. Riccio ML, Koller ML, Gilmour RF Jr. Electrical restitution and spatiotemporal organization during ventricular fibrillation. *Circ Res*. 1999;84:955–963.

38. Fenton F, Karma A. Vortex dynamics in three-dimensional continuous myocardium with fiber rotation: filament instability and fibrillation. *Chaos*. 1998;8:20–47. doi: 10.1063/1.166311.
39. Hayashi H, Shiferaw Y, Sato D, Nihei M, Lin SF, Chen PS, Garfinkel A, Weiss JN, Qu Z. Dynamic origin of spatially discordant alternans in cardiac tissue. *Biophys J*. 2007;92:448–460. doi: 10.1529/biophysj.106.091009.
40. Weiss JN, Qu Z, Chen PS, Lin SF, Karagueuzian HS, Hayashi H, Garfinkel A, Karma A. The dynamics of cardiac fibrillation. *Circulation*. 2005;112:1232–1240. doi: 10.1161/CIRCULATIONAHA.104.529545.
41. Bkaily G, Sculptoreanu A, Jacques D, Economos D, Ménard D. Apamin, a highly potent fetal L-type Ca^{2+} current blocker in single heart cells. *Am J Physiol*. 1992;262(2 Pt 2):H463–H471.
42. Paice BJ, Paterson KR, Onyanga-Omara F, Donnelly T, Gray JM, Lawson DH. Record linkage study of hypokalaemia in hospitalized patients. *Postgrad Med J*. 1986;62:187–191.
43. Dreixler JC, Jenkins A, Cao YJ, Roizen JD, Houamed KM. Patch-clamp analysis of anesthetic interactions with recombinant SK2 subtype neuronal calcium-activated potassium channels. *Anesth Analg*. 2000;90:727–732.
44. Yamamoto T, Kakehata S, Yamada T, Saito T, Saito H, Akaike N. Effects of potassium channel blockers on the acetylcholine-induced currents in dissociated outer hair cells of guinea pig cochlea. *Neurosci Lett*. 1997;236:79–82.
45. Turker I, Yu CC, Chang PC, Chen Z, Sohma Y, Lin SF, Chen PS, Ai T. Amiodarone inhibits apamin-sensitive potassium currents. *PLoS One*. 2013;8:e70450. doi: 10.1371/journal.pone.0070450.

CLINICAL PERSPECTIVE

Hypokalemia is a known risk factor for sudden cardiac death. Proarrhythmic effects of hypokalemia have been related to reduced repolarization reserve as a result of direct suppression of multiple K^+ currents and inhibition of the Na-K pump, causing increases in intracellular Ca^{2+} (Ca_i). We hypothesized that Ca_i overload in this setting may activate apamin-sensitive small-conductance calcium-activated K^+ current (I_{KAS}), attenuating the reduction in repolarization reserve and protecting against arrhythmias. In the present study, we documented that I_{KAS} was indeed upregulated during hypokalemia, especially at sites of late activation during ventricular pacing, which exacerbated Ca overload. Apamin, a specific I_{KAS} blocker, increased ventricular vulnerability to fibrillation. These findings support the notion that I_{KAS} may act as a rescue current to counteract excessive reduction in repolarization reserve during hypokalemia, reducing the risk of arrhythmias. In addition to hypokalemia, other conditions associated with reduced repolarization reserve and abnormal Ca handling such as heart failure and myocardial infarction have also been shown to increase I_{KAS}. Blocking I_{KAS} by drugs or foods might remove this rescue mechanism and make the patients more vulnerable to ventricular arrhythmias and sudden death, especially in the setting of chronic right ventricular pacing or frequent premature ventricular contractions. We conclude that I_{KAS} may be an important rescue current that helps to maintain repolarization reserve in diseased conditions and hypokalemia. These findings may be important for understanding drug safety and the detrimental effects of ventricular pacing and frequent premature ventricular contractions.

SUPPLEMENTAL MATERIAL

Methods

Optical mapping studies

Surgical preparation

The study protocol was approved by the Institutional Animal Care and Use Committee of Indiana University School of Medicine and the Methodist Research Institute, Indianapolis, Indiana. A total of 23 New Zealand white rabbits with body weight 3.5 to 5.0 Kg were used for optical mapping studies. Among them, 7 were used for normokalemic experiments, 13 for hypokalemic experiments that include 9 with right ventricular (RV) pacing and 4 with left ventricular (LV) pacing. In addition, we studied 3 hypokalemic hearts during atrial pacing. Under isoflurane general anesthesia, the hearts were harvested and Langendorff perfused with 37°C oxygenated Tyrode's solution. The composition of Tyrode's solution in normokalemic experiments (N=7) was (in mmol/L): NaCl 128, KCl 4.7, $NaHCO_3$ 24, NaH_2PO_4 1.8, $CaCl_2$ 1.8, $MgCl_2$ 1.2, glucose 11.1 and bovine serum albumin 40 mg/L with a pH of 7.40. In hypokalemic experiments (N=13), the KCL in the Tyrode's solution was decreased to 2.4 mmol/L once hearts were cannulated. We then performed radiofrequency atrioventricular (AV) node ablation to reduce the ventricular rate to < 60 bpm (ventricular escape cycle length > 1000 ms). The slow rates allowed us to study the electrophysiological effects of apamin at both fast and slow pacing rates. The pacing sites were either in the right ventricle (RV, N=16) or in the left ventricle (LV) base (N=4). All chemicals were purchased from Sigma-Aldrich (St. Louis, MO).

Optical Mapping

We performed simultaneous optical mapping of the membrane potential (V_m) and Ca_i using techniques similar to that reported elsewhere.[1] The hearts were stained with Rhod-2 AM (1.2 μmol/L, 0.18 μmol in 150 mL Tyrode's solution, from Invitrogen, Grand Island, NY) for Ca_i mapping and then RH237 (10 μmol/L, 0.4 μmol in 40 ml, from Invitrogen, Grand Island, NY) for V_m mapping. Blebbistatin (15~20 μmol/L, from Tocris Bioscience, Minneapolis, MN) was used to inhibit contraction. The hearts were excited with a laser (Verdi G5, Coherent Inc., Santa Clara, CA) at a wavelength 532 nm. The fluorescence was collected through a lens and dichroic mirror with a 650 nm cut-off wavelength. The signals were further filtered (715 mm for V_m and 580 nm for Ca_i) and recorded simultaneously with two MiCAM Ultima cameras (BrainVision, Tokyo, Japan) at 2 ms/frame temporal resolution and 100 x 100 pixels with spatial resolution of 0.35 x 0.35 mm^2 per pixel. The average fluorescence level (F) of an individual pixel was first calculated for the duration of recording. The ratio of fluorescence

$((F-F_0)/F_0)$ of the individual pixel was further filtered with 3 x 3 x 3 averaging to generate the maps.

Pseudoelectrocardiogram (pECG) was monitored using 2 electrodes placed in the left atrium and the RV, respectively. A bipolar electrode was used to pace the RV with an output at 2.5 times the diastolic pacing threshold in 9 hypokalemic and 7 normokalemic hearts. A dynamic pacing protocol was performed to determine the action potential duration restitution (APDR) curve and the optical signals were mapped at different pacing cycle length (PCL). The PCLs were progressively shortened from 1000 ms until VF was induced or the loss of 1:1 capture of the ventricles. We started to acquire optical mapping signal after at least 30 paced beats at the same PCL. A S1/S2/S3 (short/long/short) pacing protocol (S1 30 beats with S1-S1 300 ms, a long S1-S2 of 1000 ms and a S2-S3 starting from 300 ms and gradually shortened to the ventricular effective refractory period (ERP)) and long/short coupled pacing protocol (a long PCL with 1000 ms coupled with a short PCL starting from 300 ms and gradually shortened to the ventricular ERP) were used to simulate the ECG characteristics that initiates the early afterdepolarizations (EADs) and torsades de pointes (TdP) ventricular tachycardia in humans. Apamin (100 nmol/L) was then added to the perfusate and the ventricles were continuously paced at 300 ms PCL for an hour. The protocols were then repeated. An addition 4 hearts were studied during hypokalemia with LV pacing. The output was set at 2.5 times the diastolic pacing threshold and the PCL was fixed at 300 ms both at baseline and after apamin infusion. An additional 3 hearts were paced from the right atrial appendage at 300 ms PCL. Optical mapping was performed during hypokalemia at baseline. Apamin (100 nmol/L) was then added to the perfusate and the optical mapping was repeated 1 hour later.

I_{KAS} densities determined by voltage-clamp techniques

Additional rabbit hearts were used for patch clamp studies according to previously described methods.[2] Briefly, the rabbits were anesthetized with pentobarbital (50 mg/Kg) and the hearts were rapidly excised. The ascending aorta was cannulated, and the heart was retrogradely perfused with oxygenated Tyrode's solution at 37°C. After rinsing off remaining blood, the heart was perfused for 15 min with nominally Ca^{2+}-free Tyrode's solution containing collagenase II (200 U/ml; Worthington Biochemicals). Ventricles were then removed and minced into small pieces followed by dispersion with a large bore pipette. The dispersed tissue was filtered through a 100-μm Nylon mesh, the cells were resuspended in Tyrode's solution containing 100 nmol/L $CaCl_2$. The cell suspension was centrifuged at 500 rpm for 5 min at room temperature. The supernatant was removed and the cells were resuspended in a buffer containing 200 nmol/L $CaCl_2$. Centrifugation was repeated one more time and the cells were resuspended in Tyrode's solution containing 500 nmol/L $CaCl_2$ until use.

Whole-cell I_{KAS} was recorded using the voltage-clamp technique in the ruptured-patch

configuration.[3] The extracellular solution contained (in mmol/L): N-methylglucamine (NMG) 140, $MgCl_2$ 1, glucose 5, HEPES 10 (pH 7.4 using HCl), and KCl 4.7 or 2.4. The internal solution consisted of (in mmol/L): potassium gluconate 144, $MgCl_2$ 1.15, EGTA 5, HEPES 10, and $CaCl_2$ yielding a free Ca^{2+}-concentration of 1 µmol/L [Ca-EGTA Calculator v1.3 (http://maxchelator.stanford.edu/CaEGTA-TS.htm)]. All experiments were carried out at room temperature. Pipette resistances ranged from 1-1.5 MΩ when filled with the pipette solution. After achieving a gigaseal, the test-pulse current was nulled by adjusting the pipette capacitance compensation. After break-in, the whole-cell charging transient was nulled by adjusting whole-cell capacitance and series resistance. Series resistance was compensated by 70 - 80%. After obtaining whole-cell access, the cell was dialyzed for 15 min before the start of current recordings. Currents were elicited using a voltage-ramp from +40 to -100 mV (0.35 mV/s) from a holding potential of -50 mV. Voltage-ramps were repeated every 10 s. Once the currents had stabilized, the cell was exposed to the same bath solution supplemented with apamin (100 nmol/L). Currents recorded in the presence of apamin were digitally subtracted from those measured in its absence and the density of the apamin-sensitive current at 0 mV was calculated.

Data Analysis

APD_{80} was measured at the level of 80% repolarization of the action potential. The mean APD_{80} was calculated for all available ventricular pixels. The F/F_0 ratio was used to estimate the relative concentration of Ca_i[4] between normokalemia and hypokalemia and between early and late activation sites. Continuous variables are expressed as mean and 95% confidence interval (CI). Paired Student's t-tests were used to compare continuous variables measured at baseline and during apamin infusion. Non-parametric Mann-Whitney-Wilcoxon test was used to compare the I_{KAS} current densities with 4.7 mmol/L and 2.4 mmol/L potassium concentration in the Tyrode solution. Comparison of prevalence of VF inducibility between baseline and during apamin infusion was performed using Fisher's exact test. A 2-sided $P \leq 0.05$ was considered statistically significant.

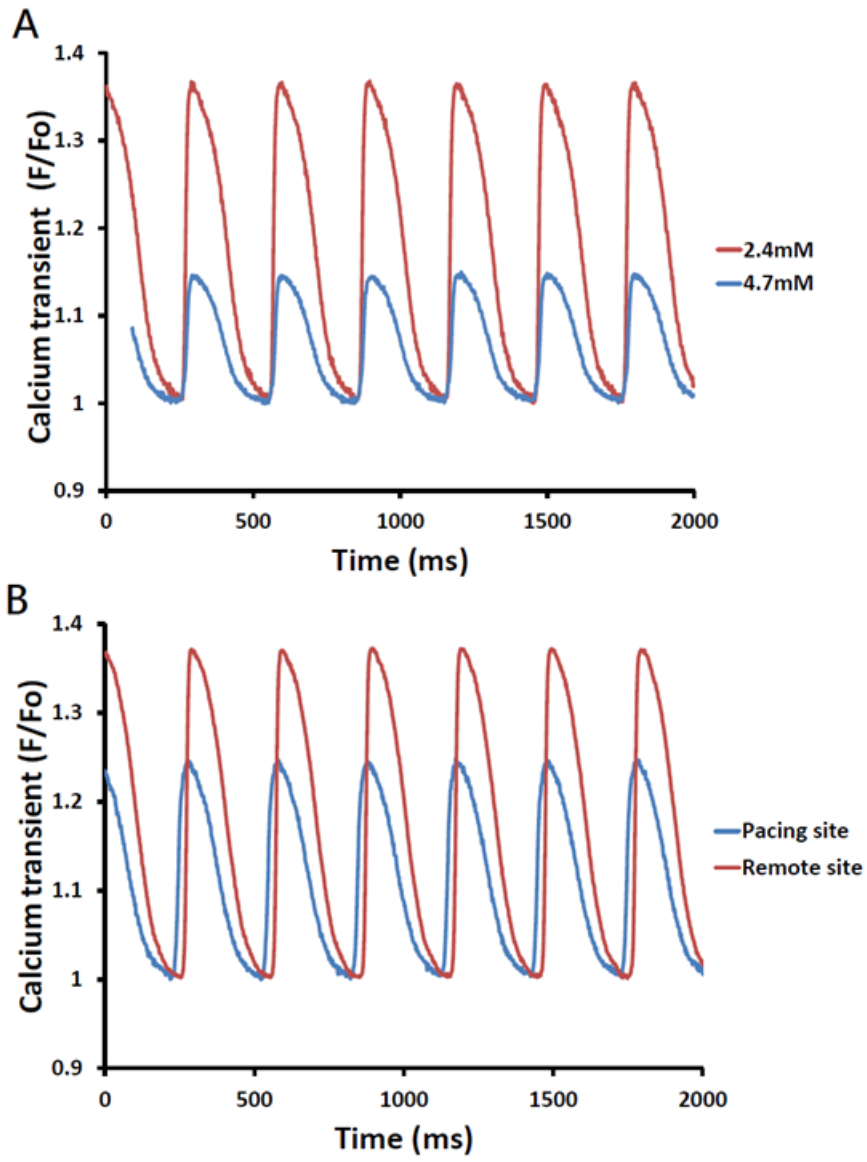

Figure 1. Effect of extracellular $[K^+]_o$ concentration and activation sequence on Ca^{2+} transient. **Panel A** shows representative Ca^{2+} transient in ventricles at two different K^+ concentrations. The F/F_0 was much higher with 2.4 mmol/L $[K^+]_o$ than with 4.7 mmol/L $[K^+]_o$ in the Tyrode solution. **Panel B** shows representative tracings of Ca^{2+} transient at two different sites on one ventricle perfused with low (2.4 mmol/L) $[K^+]_o$ Tyrode solution with PCL of 300 ms. The F/F_0 in the late activation site (remote site) was much higher than that at the early activation site (near pacing site). F = fluorescence of calcium transient; F_0 = fluorescence of calcium transient during late diastole. PCL = pacing cycle length.

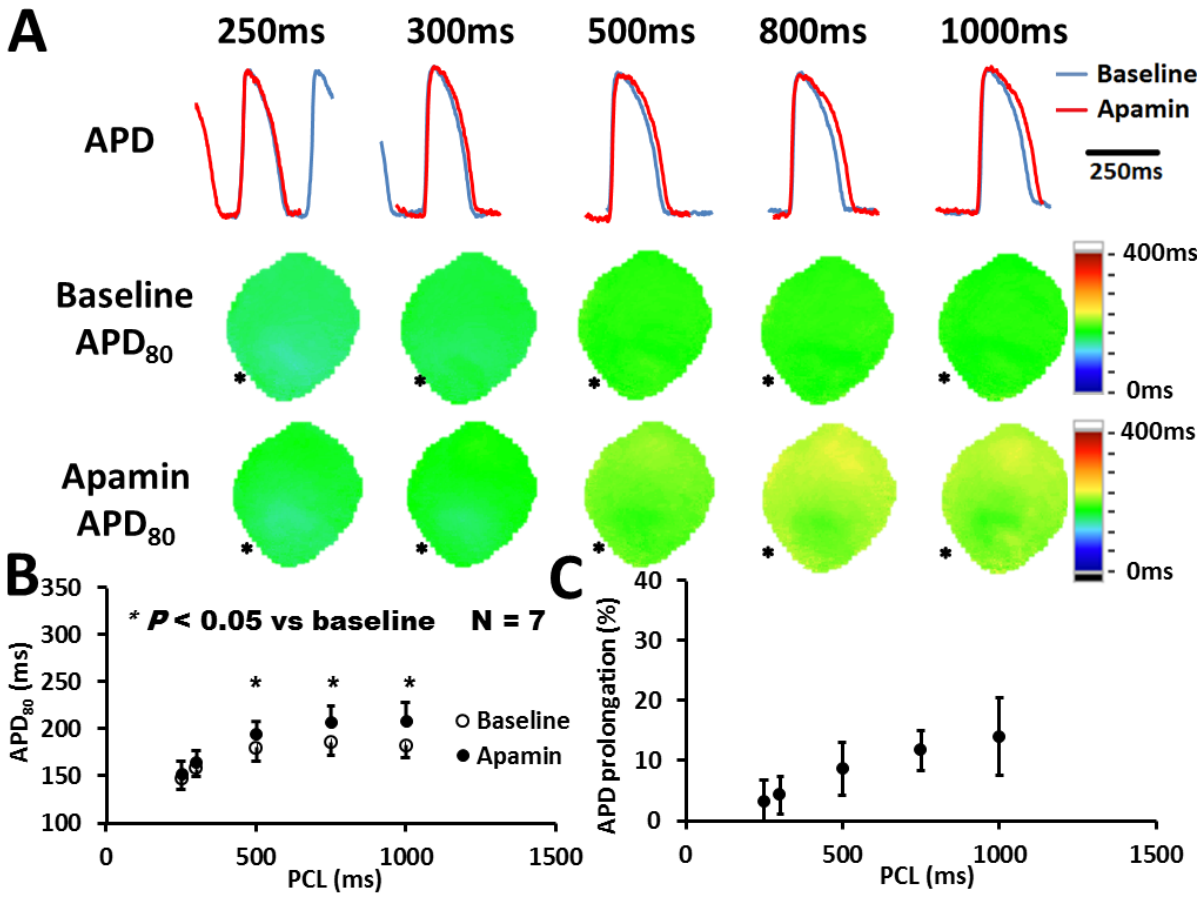

Figure 2. Effects of I_{KAS} blockade on APD at different PCLs in normokalemic (4.7 mmol/L) ventricles. A, Representative V_m traces and APD_{80} maps at baseline and in the presence of apamin (100 nmol/L). The magnitude of APD prolongation was more prominent at long PCLs than at short PCLs. The pacing site (asterisk) was located at RV apex. B, Apamin significantly prolonged APD_{80} at 500, 800, and 1000 ms PCLs, and the prolongation was more prominent at longer PCLs. *P < 0.05. C, A plot of ΔAPD_{80} ratio [(APD_{80} after apamin - APD_{80} at baseline)/APD_{80} at baseline] vs PCL shows that apamin prolonged APD_{80} by approximately 14% at a PCL of 1000 ms but only by 3% at a PCL of 250 ms. APD = action potential duration; I_{KAS} = apamin sensitive small conductance calcium activated potassium current; PCL = pacing cycle length.

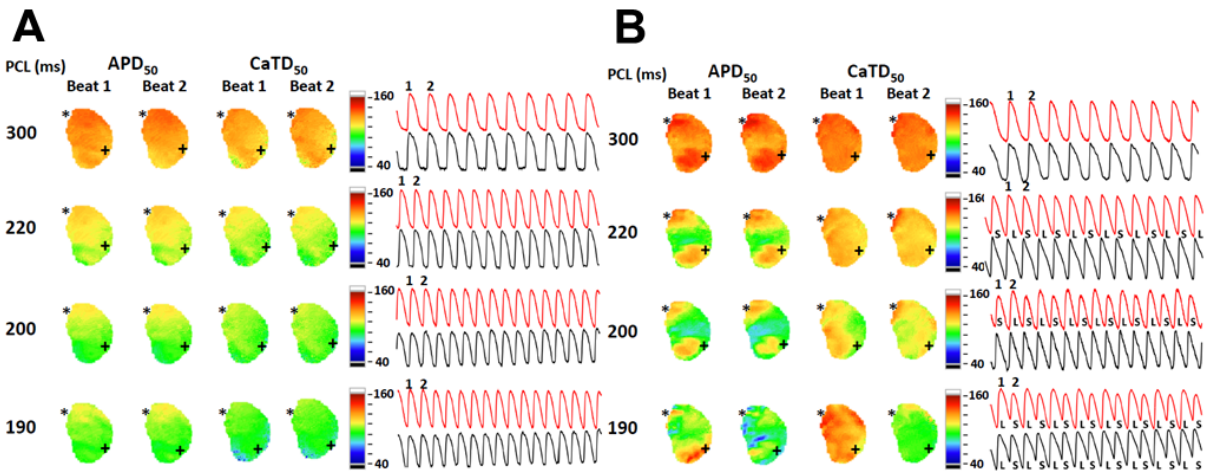

Figure 3. Effects of PCL on CaTD alternans. A shows no alternans when PCL shortened from 300 ms to 190 ms when the extracellular $[K^+]_o$ concentration was 4.7 mmol/L. B shows the development of CaTD alternans at 220 ms PCL at $[K^+]_o$ concentration of 2.4 mmol/L. The APD alternans was observed only when PCL was shortened to 190 ms. The area of APD alternans was much smaller than the area of CaTD alternans. The pacing site on the RV was marked by an asterisk. The optical signal was recorded from the site marked by a plus sign, which is remote from the site of the pacing. The red and black tracings indicated the calcium and voltage signals, respectively. APD = action potential duration; CaTD = calcium transient duration; L = long; PCL = pacing cycle length; S = short.

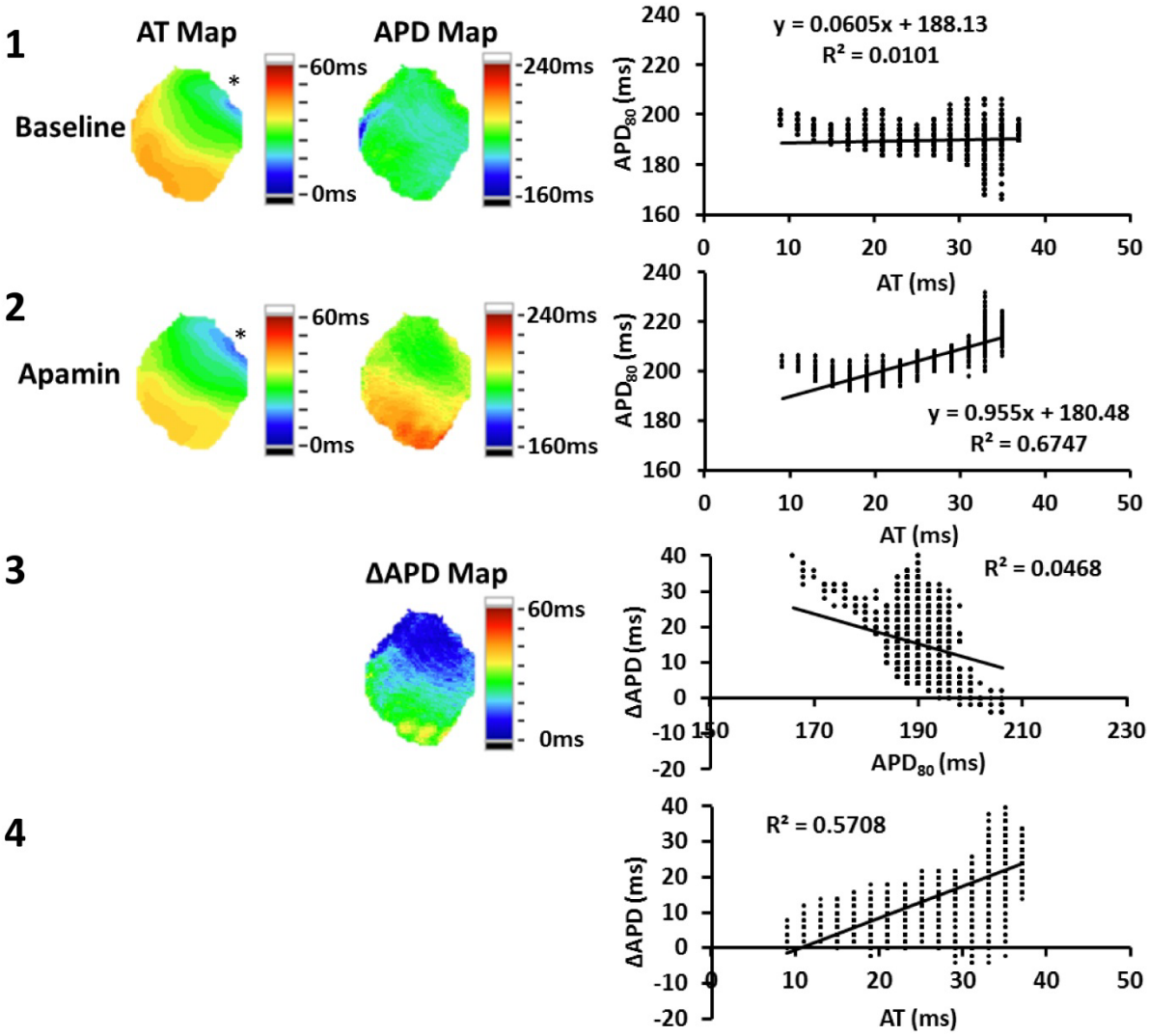

Figure 4. Effects of I_{KAS} blockade on epicardial action APD-to-AT relationship determined during LV basal pacing with PCL 300 ms in hypokalemic (4.7 mmol/L) ventricles. The top two rows show the AT maps, APD maps and corresponding plot of APD-AT relationship at baseline **(1)** and after apamin **(2)** infusion in one ventricle during 300 ms PCL. The pacing site (asterisk) is located at LV base. Apamin increased the slope of APD-AT from 0.06 to 0.95. **(3)** The ΔAPD map and correlation between ΔAPD and baseline APD_{80} in the ventricle at PCL 300 ms. **(4)** The corresponding plot of ΔAPD-AT at PCL 300 ms. APD = action potential duration; AT = activation time; I_{KAS} = apamin sensitive small conductance calcium activated potassium current; LV = left ventricle; PCL = pacing cycle length; ΔAPD = APD_{80} after apamin - APD_{80} at baseline.

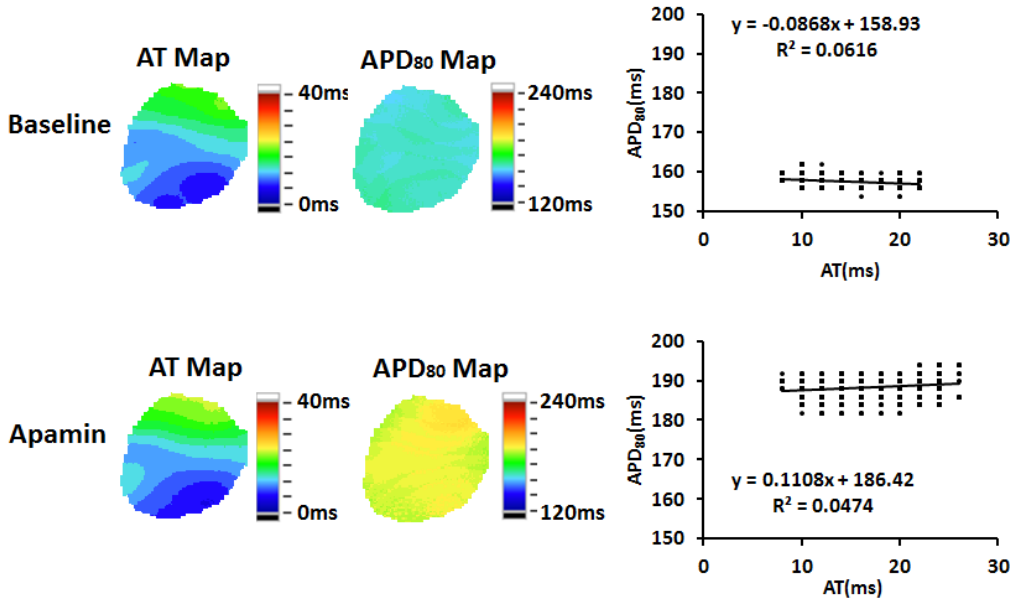

Figure 5. Effects of apamin (100 nmol/L) on atrially paced hearts. The experiment was done at 300 ms PCL and 2.4 mmol/L $[K^+]_o$. Apamin increased the ventricular APD in this and two additional hearts studied. The sequence of activation on the epicardium remained stable. APD = action potential duration; AT = activation time; PCL = pacing cycle length

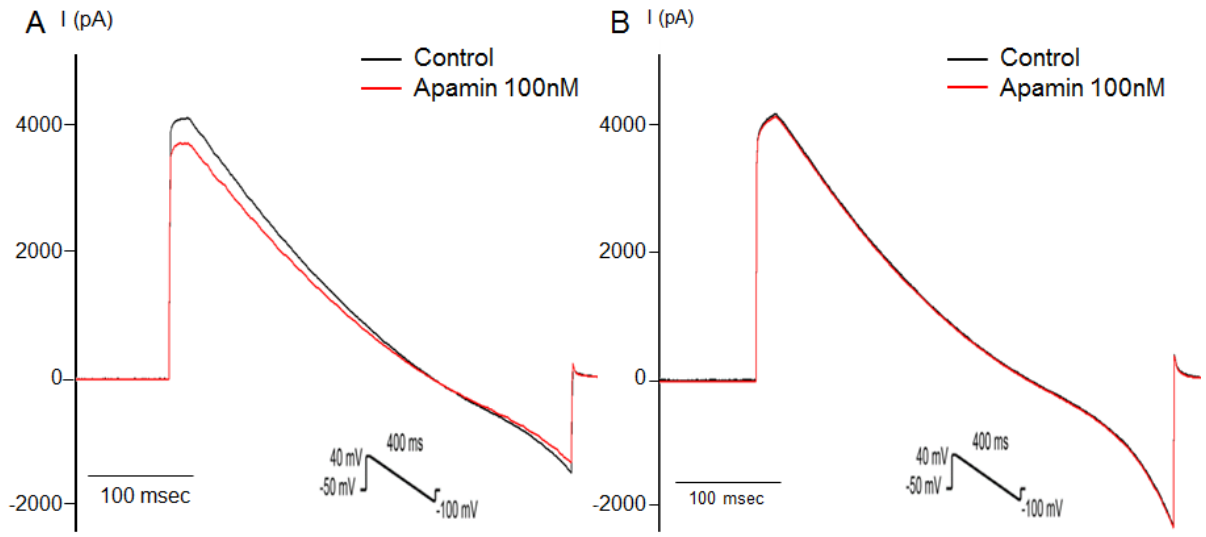

Figure 6. Densities of I_{KAS} at low and normal extracellular K^+ concentration in isolated ventricular myocytes. A shows the effects of apamin on K^+ currents at 2.4 mmol/L $[K^+]_o$. The differences between Control tracing and Apamin tracing is the apamin-sensitive K^+ current (I_{KAS}). B shows an absence of I_{KAS} when the $[K^+]_o$ concentration was 4.7 mmol/L.

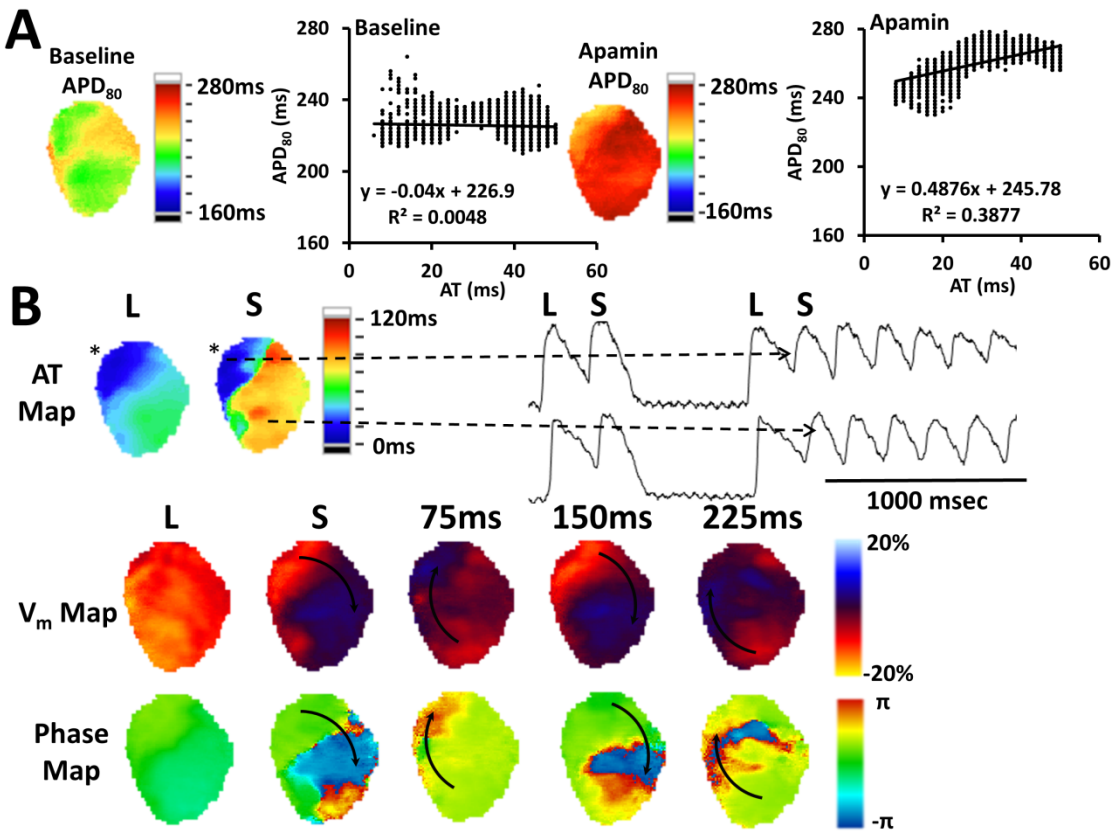

Figure 7. Induction of reentry and VF by long/short (L/S) pacing protocol during hypokalemia, after I_{KAS} blockade. **A,** APD maps and the corresponding APD-to-AT relationship from the representative ventricle at baseline and after apamin infusion. Map were generated at the PCL of 1000 ms. **B,** Representative sustained ventricular arrhythmia (VF) induced by L/S (1000/230 ms) coupled pacing protocol. The pacing site is located at RV base (asterisk). The premature contraction (S) led to ventricular activation near pacing site (blue) and local conduction block leading to delayed activation remote from pacing (red). The voltage (V_m) map at the bottom shows conduction block in the center and activation circling the periphery of the blocked region (arrows). The phase map shows the development of phase singularities at the site of block, causing reentry that initiates VF. APD = action potential duration; AT = activation time; I_{KAS} = apamin sensitive small conductance calcium activated potassium current. L = long; S = short.

References

1. Chang PC, Hsieh YC, Hsueh CH, Weiss JN, Lin SF, Chen PS. Apamin induces early afterdepolarizations and torsades de pointes ventricular arrhythmia from failing rabbit ventricles exhibiting secondary rises in intracellular calcium. *Heart Rhythm*. 2013;10:1516-1524
2. Ahmmed GU, Xu Y, Hong Dong P, Zhang Z, Eiserich J, Chiamvimonvat N. Nitric oxide modulates cardiac Na(+) channel via protein kinase A and protein kinase G. *Circ Res*. 2001;89:1005-1013
3. Yu CC, Ai T, Weiss JN, Chen PS. Apamin does not inhibit human cardiac Na+ current, L-type Ca2+ current or other major K+ currents. *PLoS One*. 2014;9:e96691
4. Tsai CT, Wang DL, Chen WP, Hwang JJ, Hsieh CS, Hsu KL, Tseng CD, Lai LP, Tseng YZ, Chiang FT, Lin JL. Angiotensin II increases expression of α1C subunit of L-type calcium channel through a reactive oxygen species and cAMP response element-binding protein-dependent pathway in HL-1 myocytes. *Circ Res*. 2007;100:1476-1485

Small-Conductance Calcium-Activated Potassium Current Is Activated During Hypokalemia and Masks Short-Term Cardiac Memory Induced by Ventricular Pacing

Yi-Hsin Chan, Wei-Chung Tsai, Jum-Suk Ko, Dechun Yin, Po-Cheng Chang, Michael Rubart, James N. Weiss, Thomas H. Everett IV, Shien-Fong Lin and Peng-Sheng Chen

Circulation. 2015;132:1377-1386; originally published online September 11, 2015;
doi: 10.1161/CIRCULATIONAHA.114.015125
Circulation is published by the American Heart Association, 7272 Greenville Avenue, Dallas, TX 75231

Print ISSN: 0009-7322. Online ISSN: 1524-4539